University of Szeged
Faculty of Science and Informatics
Doctoral School of Geosciences
Department of Physical Geography and Geoinformatics

Landslide hazard assessment using advanced remote sensing techniques and GIS

Thesis of dissertation

Muhannad Hammad

Supervisors

Dr. Mucsi László — **Associate professor**

Dr. Boudewijn van Leeuwen — **Assistant professor**

Szeged

2020

1. Introduction and objectives

Geohazards are natural phenomena containing all the different geological processes and geographical features that are capable of triggering catastrophic events or natural disasters that threaten human beings and damage property, critical infrastructure and the natural environment. Since landslides are an important type of geohazards, it is necessary to assess and map the susceptibility of a region to landslides and the hazard of landslides with the highest available spatial and temporal resolution.

Landslide investigation has been developed providing remarkable results through the integration of remote sensing data and Geographic Information System (GIS) using different statistical analysis models to investigate landslide susceptibility zones (Biswajeet and Saro, 2007).

Some approaches have already considered the use of Interferometry Synthetic Aperture Radar (InSAR) techniques for providing information on slope stability by analysing the total value and velocity of these ground-surface deformations. The most effective approaches of using interferometry for investigating ground-surface deformations have applied mainly the Differential InSAR (D-InSAR) and Persistent Scatterer Interferometry (PSI) techniques (Gabriel et al., 1989; Hooper, 2006).

The road network in northwest Syria is susceptible to unforeseen landslides. Several roads have been damaged by landslides annually after intense rainfall events. These unpredicted landslides and the resulting damage to the road network threaten the lives and properties of the people who live there and cause both direct and indirect losses. Therefore, the area in northwest Syria needs comprehensive landslide hazard assessment, leading to produce a landslide hazard map and identify potential landslide areas to be taken into account by the authorities in order to guide the regional planning processes and minimize the risk in those areas.

The aim of this research was to *develop a workflow for the creation of the landslide hazard map* for northwest Syria that can be updated regularly to identify all sites with a high hazard for landslides throughout the area and along the road network, in particular along the highway there. This will help local authorities to take the necessary precautions at all these sites to avoid losses due to possible future landslides along the highway. Based on the research aim, the following main objectives have been achieved:

- I have determined the *relative influence of each causative factor* on the occurrence of landslides in northwest Syria according to the statistical analysis process to find out the most factors influencing and controlling the spatial distribution of landslides there.

- I have verified the *efficiency of the four different statistical analysis methods* applied in this research for predicting landslide susceptibility to find out which method gives better landslide susceptibility results than the others in order to pick out the optimal landslide susceptibility map of northwest Syria.
- I have also evaluated the *capability of Sentinel-1 SAR data* to generate digital elevation models and to measure mean velocities of ground-surface deformations in northwest Syria and to investigate the advantages and disadvantages of both purposes.
- I have assessed the *landslide hazard using a landslide hazard matrix* based on landslide susceptibility and ground-surface deformation intensity resulting from the mean velocity data of the PSI technique to determine the spatial distribution of the low, medium and high hazard zones for landslides along the road network and to identify the sites along the highway that could be considered high hazard areas for landslides.

2. Study area

2.1 Geographical and climatic conditions

The study area covers an area of 264.58 km2 from 35.75◦ in the south to 35.94◦ at the Turkish border in the north, and from 36.00◦ in the east to 35.80◦ at the Mediterranean Sea in the west. The elevation is between 0 and 1130 metres above sea level. The highest average monthly rainfall is around 125 mm in both December and January, while the maximum monthly rainfall reached 379 mm in January 2012 and the maximum annual rainfall reached 1284 mm in 2012 (NASA-POWER, 2019).

2.2 Geological conditions

The study area contains the Baer-Bassit ophiolite complex deposits in addition to the Phanerozoic sedimentary rocks.

The lithology of the sedimentary deposits consists of pelagic and neritic carbonate, radiolarian chert, conglomerate, clayey and sandy deposits.

The ophiolite complex outcrop is dominated by two massifs, Baer in the east and Bassit in the west. The Baer massif rocks is relatively structurally intact, while the Bassit massif rocks are over-thrusted by thin imbricate thrust sheets of pillow lavas (Al-Riyami et al., 2000). Baer-Bassit ophiolite complex was originally described by Dubertret in 1955 and mapped by Kazmin and Kulakov in 1968 who have determined the following units in the Syrian Baer-Bassit ophiolite complex: metamorphic sole, ultrabasic and basic rocks, volcanic sedimentary rocks.

3. Methods

3.1 Digital elevation model generation

The DEM was generated using two different approaches for two different purposes. The first DEM, the topography-based DEM, was created on the basis of a topographical map from 1984 and was used to represent the topographical characteristics of the area as they were before the occurrence of the landslides under investigation and to extract the derivative maps involved in the statistical analysis of landslide susceptibility, i.e. slope gradient, slope aspect, terrain curvature and drainage network. The second DEM, the SAR-based DEM, was created on the basis of Sentinel-1 data and used as a newer and higher-resolution DEM for the PSI technique applied in this research.

3.2 Landslide inventory map preparation

The landslide inventory map was prepared based on all available geotechnical reports as well as information from the authorities and the local population about past landslides to determine the location of each of these landslides. The spatial extent of these landslides in the landslide inventory map was checked individually and verified by a visual comparison between the Landsat-5 TM image of 22 September 1984 and the Landsat-8 OLI image of 6 October 2018 with help of ancillary information available through the Historical Imagery tool in Google Earth. The Historical Imagery tool in Google Earth was also used to detect changes in texture and characteristics of ground-surface and vegetation cover during this period and to verify whether these changes are indicators of past landslide events or just changes due to human activity or some fire events that occurred during this period, especially after 2011 when the war in Syria began.

The resulting landslide polygons were randomly divided into two sets; 70% of all landslide polygons was used as a training set for the statistical analysis methods used in this research to create the landslide susceptibility maps, and the remaining 30% was used as a testing set to validate the resulting susceptibility maps.

The same procedure was carried out for the non-landslide dataset which was prepared with the same size of the landslide dataset to optimally perform the statistical analysis of the landslide susceptibility. Thus, the non-landslide dataset was prepared with the same number of polygons and the same number of pixels as a whole, based on relevant geotechnical reports and maps as well as personal knowledge from local field work.

3.3 Causative factor maps preparation for susceptibility analysis

For statistical analysis of susceptibility to landslides, nine causative factors influencing the spatial distribution of landslides were taken into account depending on various criteria such as mapping unit and type of landslides in the area, as well as the availability of data and the results of many similar studies (Guzzetti, 2005; Pradhan et al., 2011; Lee et al., 2012). These factors are: slope gradient, slope aspect, terrain curvature, distance to streams, distance to roads, distance to faults, lithology, land cover, and Normalized Differential Vegetation Index (NDVI).

Within the relatively small study area, it is very likely that the amount of rainfall is the same throughout the area according to the available rainfall data. Therefore, it was decided to exclude rainfall data from the statistical analysis of landslide susceptibility. After all, rainfall can be considered as a trigger rather than a causative factor for landslide occurrence in the area.

The preparation process of the nine causative factor maps was done separately on the basis of the source data of each causative factor. In ArcGIS, the causative factor maps were prepared as a raster grid format, and clipped to the same spatial extent. Then, all resulting raster maps were reprojected using the same coordinate system, and resampled to the same pixel size to make them uniform. The pixel size for all the map layers was set to 12.5 m, which is the recommended grid resolution of the topography-based DEM. In order to be used in the landslide susceptibility analysis, each of the nine causative factor maps was reclassified into number of classes depending on its own criteria.

3.4 Landslide susceptibility mapping using statistical analysis

In ArcGIS, the training set extracted from the landslide inventory map was converted to a raster set. Then, the training set was spatially linked to each of the causative factor maps to determine within each factor the class corresponding to each pixel of the training set, thus allowing to perform a susceptibility statistical analysis and produce a landslide susceptibility map according to each of the four statistical methods applied.

At the end, each landslide susceptibility map resulting from the different statistical analysis methods was validated using the Area Under the Curve (AUC) analysis. The landslide susceptibility map with the best AUC, was selected as the final landslide susceptibility map (Figure 1).

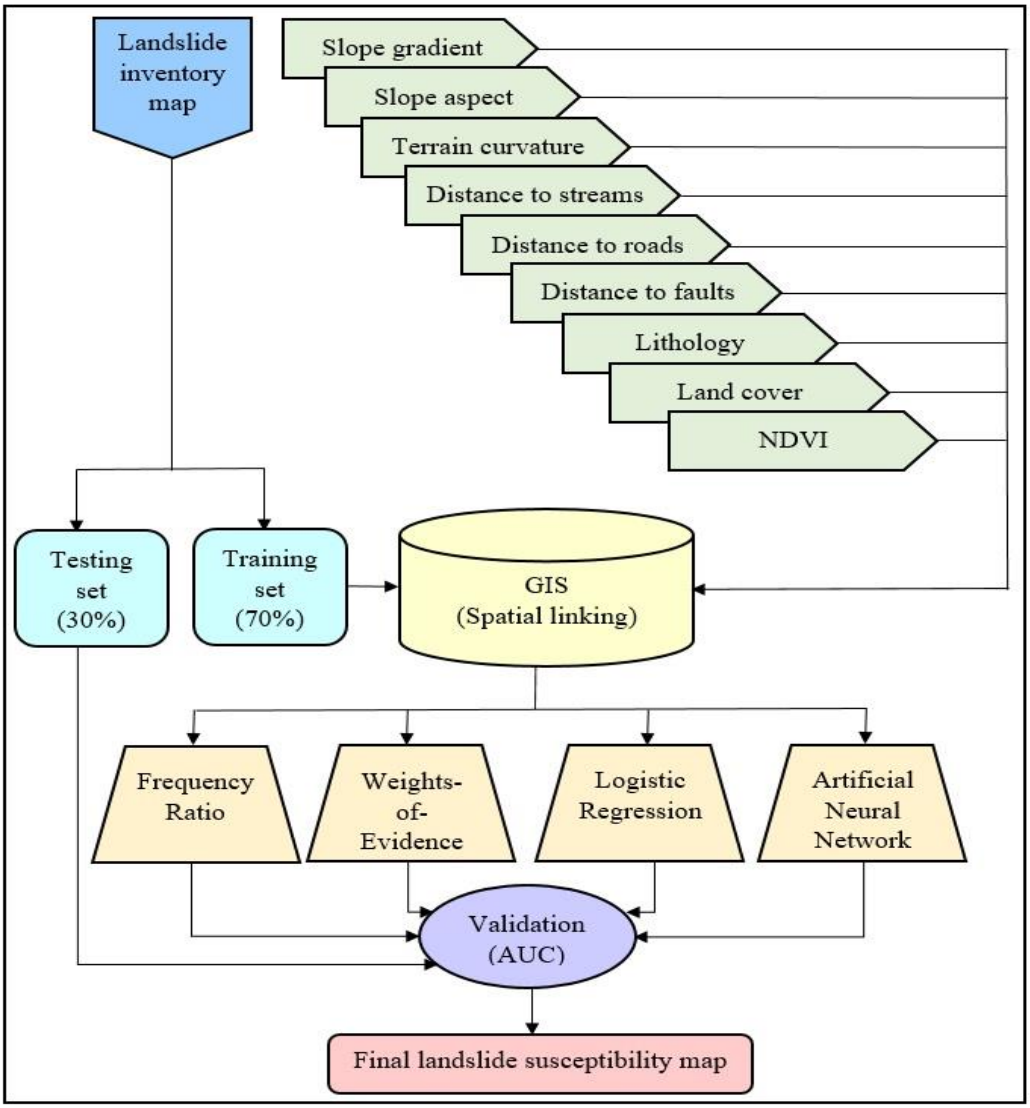

Figure 1: Methodology of landslide susceptibility mapping.

3.5 Ground-surface deformation mapping using advanced remote sensing techniques

Ground-surface deformation mapping using advanced remote sensing techniques was carried out for a period between October 2018 and March 2019 to cover the majority of a rainfall season. Two advanced remote sensing techniques were applied. The first was the Persistent Scatterer Interferometry (PSI) which was used to create the mean velocity map of ground-surface deformations in the satellite LOS direction during the study period. The second was the Differential InSAR (D-InSAR) which was used to create the map of total ground-surface deformations in the satellite LOS direction during the same period to be used in the validation of interferometry results by comparison with D-GPS field measurements.

3.5.1 Mean velocity map of ground-surface deformations using PSI technique

Fourteen images were co-registered in SNAP software to one unique master image chosen from them using the Sentinel-1 toolbox. The thirteen resulting master-slave pair images with different temporal and perpendicular baselines were also processed in SNAP to generate two final products for all pair images with and without interferogram formation. The two final products are required to export the combination of amplitude and wrapped phases of these SAR time-series images to StaMPS in order to unwrap all the wrapped phases using advanced logarithms, as well as to estimate the Persistent Scatterer (PS) probability for each pixel in their interferograms.

As the result, a multipoint data set of all persistent scatterers with the mean velocity values was generated, representing the ground-surface deformations over the study area during the study period.

3.5.2 Total ground-surface deformations using D-InSAR technique

To create a total ground-surface deformation map using D-InSAR technique, two SAR images acquired by Sentinel-1B on 16 October 2018 and 21 March 2019 were co-registered as master and slave and used to generate an interferogram. Then, both of the flat-earth phase and the topographic phase were subtracted from the interferogram and all the necessary steps were performed to prepare the remaining displacement phase to be exported to SNAPHU. After unwrapping process in SNAPHU, the resulting unwrapped displacement phase was imported back into SNAP and converted into displacement values.

The final projected result of the total ground-surface deformations was exported as a raster grid format to ArcGIS, so that the D-InSAR results along the highway in the Balloran Dam area could be compared with the D-GPS field measurements carried out there.

3.5.3 Comparison of interferometry results with D-GPS field measurements

For D-GPS field measurements, two campaigns with the Leica System 550 GPS were conducted in October 2018 and March 2019 to obtain elevation data from 10 validation points along the highway in the Balloran Dam area, to investigate the ground-surface deformation there between 16 October 2018 and 21 March 2019. A shapefile was created from the difference values between the two campaigns at each validation point to compare the D-GPS deformation values at these ten validation points with the corresponding D-InSAR deformation values.

3.6 Landslide hazard assessment

The assessment of landslide hazard was carried out using a landslide hazard matrix (Hürlimann et al., 2008; Lu et al., 2014). The landslide hazard matrix focuses mainly on two parameters: the first is the probability of landslide occurrence, i.e. the landslide susceptibility, and the second is the intensity of ground-surface deformations, i.e. the mean velocity of ground-surface deformations during the study period, to classify the landslide hazard as low, moderate and high (Figure 2).

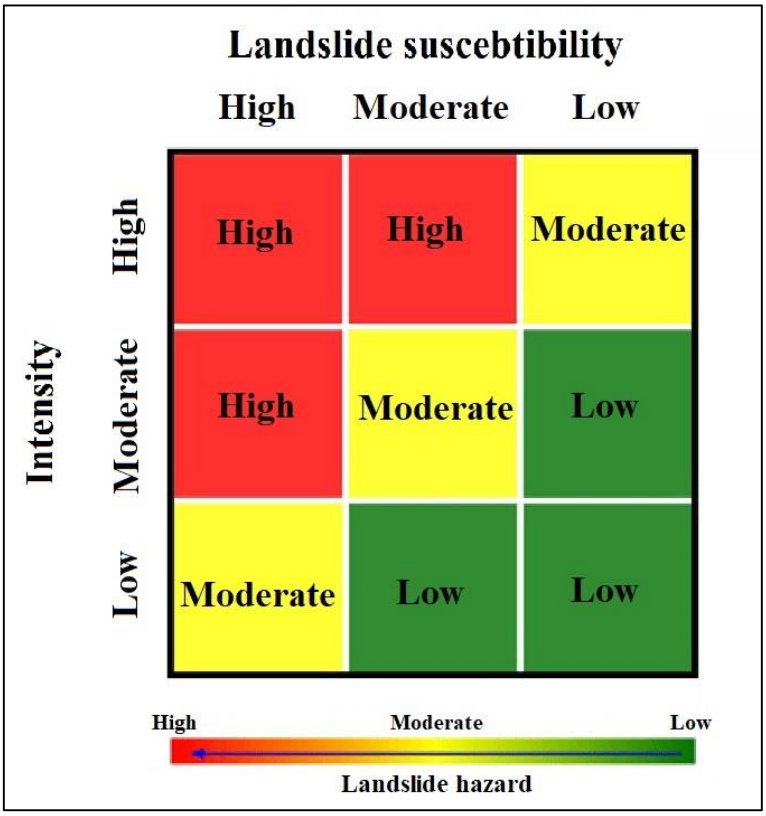

Figure 2: The landslide hazard assessment based on the landslide hazard matrix (after Lu et al., 2014).

The intensity map of the ground-surface deformations was created by interpolating the resulting multipoint data set of positive and negative mean velocities of ground-surface deformations in the LOS direction to create a mean velocity raster map. The mean velocity raster map was then reclassified into three positive mean velocity levels and three negative mean velocity levels using the Equal Interval classification method, so that the same levels were compiled to obtain the intensity map with the low-moderate-high intensity zones. At the end, the intensity map and the landslide susceptibility map were used in the landslide hazard matrix to obtain the landslide hazard map as the final result (Figure 3).

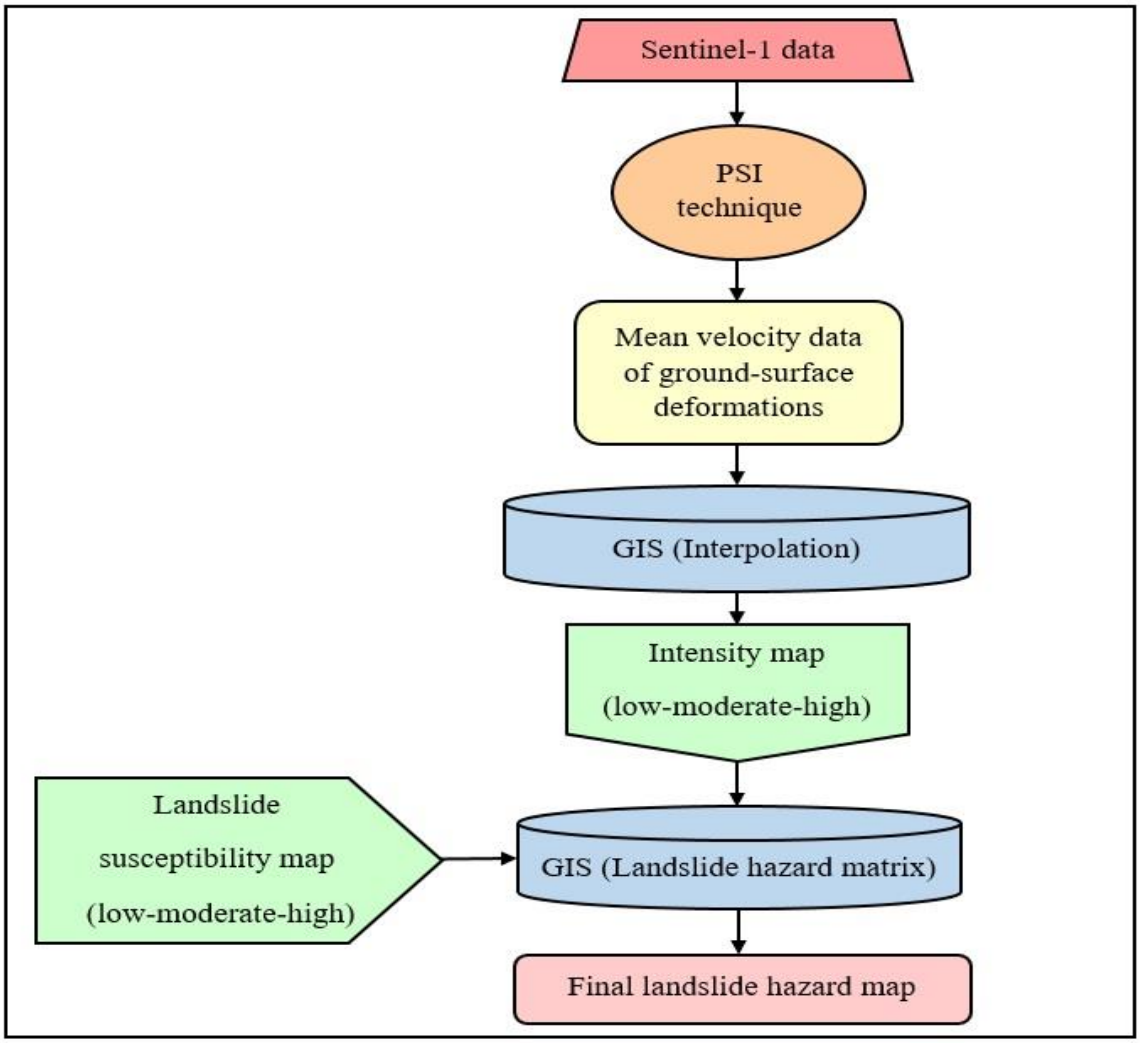

Figure 3: Methodology of landslide hazard assessment.

The interpolation of the mean velocities was performed using the Inverse Distance Weighted (IDW) interpolation in ArcGIS to obtain a continuous spatial extent from the generated mean velocity data of the ground-surface deformations (García-Davalillo et al., 2013; Notti et al., 2014).

4. Results and conclusions

4.1 ***I have developed a workflow to create the landslide hazard map using freely available Sentinel-1 data, advanced remote sensing techniques and GIS.*** The landslide hazard was assessed according to a landslide hazard matrix based on both the landslide susceptibility result of the statistical analysis process and the mean velocity result of ground-surface deformations during the main rainfall season of 2018-2019 using PSI technique (Hammad et al., 2020). the workflow of this research can be followed to monitor the landslide hazard along the road network in other places around the world, especially in areas with high rainfall and frequent landslides.

4.2 ***I have shown that different statistical analysis methods for predicting landslide susceptibility produce different results.*** Four statistical analysis methods for predicting landslide susceptibility were performed based on landslide and non-landslide training sets and nine causative factors influencing the spatial distribution of landslides, including slope gradient, slope aspect, terrain curvature, distance to streams, distance to roads, distance to faults, lithology, land cover and Normalized Differential Vegetation Index (NDVI). As a result, four different landslide susceptibility maps were produced.

4.3 ***I have found that according to the results of the FR, WoE and LR statistical analysis methods, the most influential causative factor was land cover***. Within land cover factor, the soil and agriculture land class and the built-up area class have the largest influence on the occurrence of landslides. In addition to land cover, lithology and slope gradient were also factors that significantly influenced the spatial distribution of landslides in northwest Syria.

4.4 ***I have demonstrated the need to preserve the remaining forests and vegetation areas in northwest Syria.*** The statistical analyses show that forests reduce the likelihood of landslides, but the reduction in forest and vegetation area in the Syrian coastal region reached 25.66% between 1987 and 2017 (Hammad et al., 2018a).

4.5 ***I have revealed that according to the validation results of the landslide susceptibility analysis methods using AUC analysis, the use of the ANN method in northwest Syria has achieved excellent results in terms of susceptibility to landslides.*** In contrast, the use of the FR, WoE and LR methods have achieved very good and good results (Figure 4) according to the literature (Silalahi et al., 2019). Therefore, the optimal method for creating the landslide susceptibility map in northwest Syria was the ANN method.

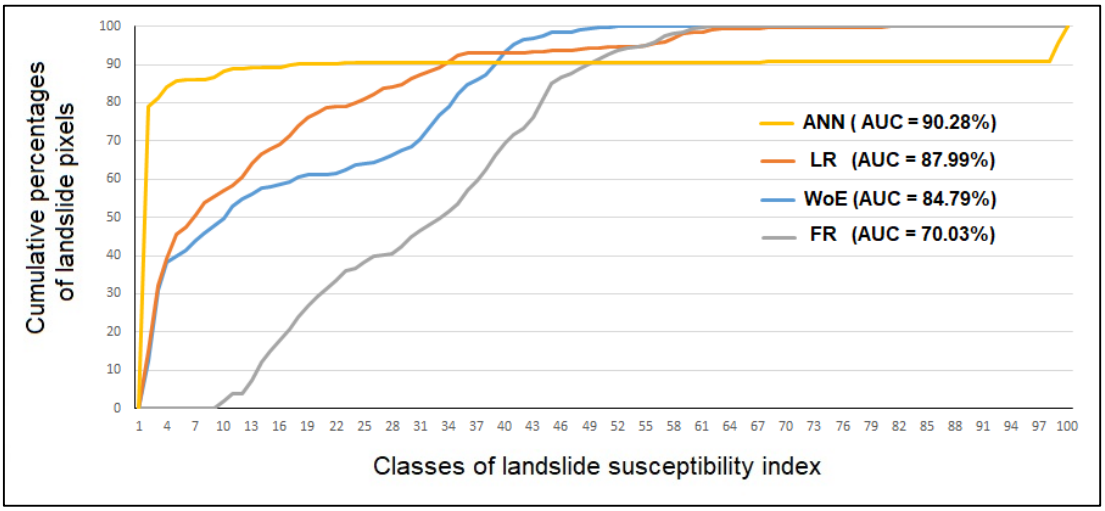

Figure 4: The AUC of the four statistical analysis methods used.

4.6 ***I have created the first landslide susceptibility map for northwest Syria with 90.28% prediction accuracy based on the ANN method (Figure 5) (Hammad et al., 2020).*** The structure of 9 input layers, 5 hidden layers and 2 output layers was selected for the neural network training phase (Figure 6), with setting up a random subdivision of the input landslide and non-landslide training dataset into 70% for training, 15% for validation and 15% for testing (Figure 7). The best performance of the neural network used for the statistical analysis of landslides was after 23 iterations (Figure 8).

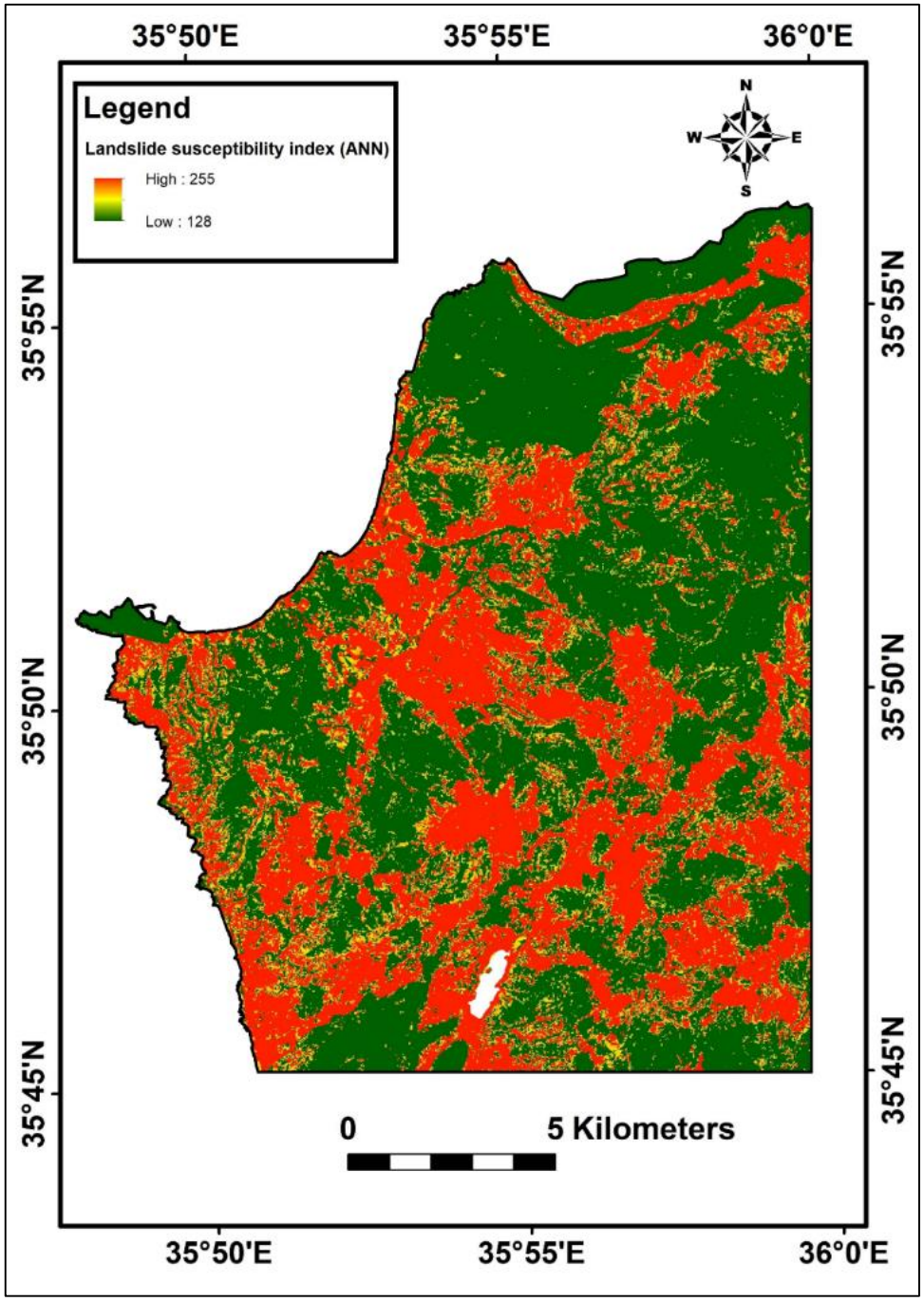

Figure 5: The landslide susceptibility map based on the ANN method.

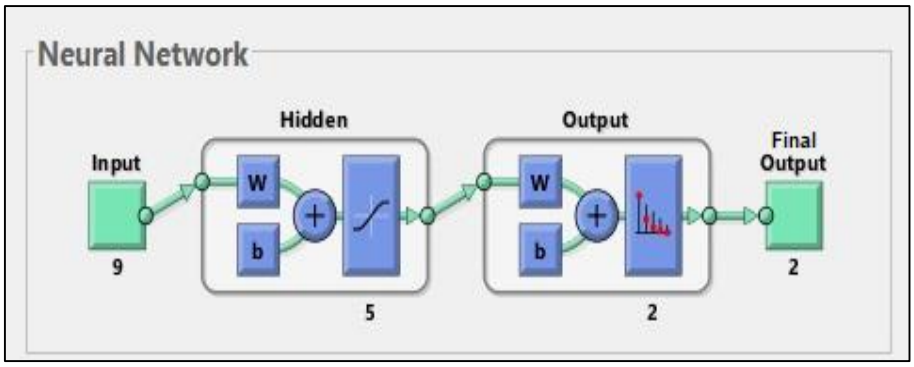

Figure 6: The structure of the neural network training used in this research.

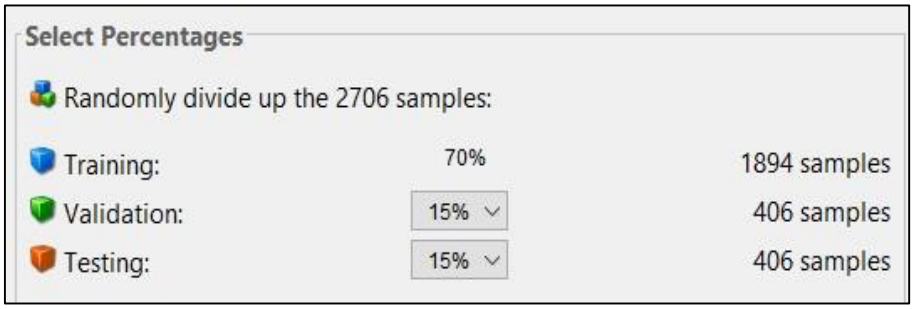

Figure 7: Input training data subdivision during the training phase in the ANN analysis.

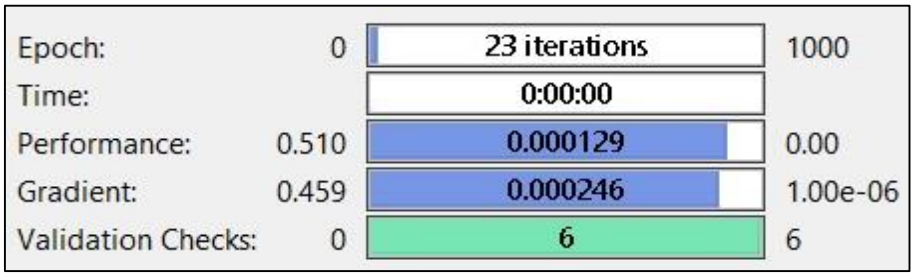

Figure 8: The performance of the neural network used for the susceptibility analysis.

4.7 ***I have demonstrated the capability of Sentinel-1 data and inSAR techniques to generate high resolution digital elevation models (Hammad et al., 2017) and also to detect and measure millimetre mean velocities of ground-surface deformation (Hammad et al., 2018b; 2020).*** However, the use of Sentinel-1 data to measure and monitor ground-surface deformations and landslides using PSI technique has proven to be more reliable and recommended than the use of this data to generate DEMs, especially when there is atmospheric inhomogeneity or in areas of dense vegetation where a large amount of decorrelation and low coherence can be generated between the two SAR images used in the DEM generation process, resulting in significant errors in the final result.

4.8 ***I have found that the comparison process between the D-InSAR displacement results and the D-GPS displacement results showed differences at 10 validation points along the highway in the Balloran area, where the root mean square of the differences was 20.14 cm (Hammad et al., 2019).*** This is because the D-GPS measurements are made in the vertical direction and the interferometric measurements are made in the LOS direction. The difference was considerable where the ground-surface deformation or landslide occurred parallel to the satellite azimuth direction and perpendicular to the LOS direction. However, the interferometric results can show us places where severe ground-surface deformations have occurred, which is adequate for the purpose of landslide hazard assessment (Table 1).

Table 1: Differences between the results of D-InSAR and D-GPS at the validation points in the Balloran area and the root mean square of these differences.

Validation point name	D-InSAR results (cm)	D-GPS results (cm)	Difference values (cm)
P1	10.64	3.10	7.54
P2	12.97	2.04	10.93
P3	16.20	75.07	58.87
P4	12.83	5.06	7.77
P5	10.77	3.12	7.65
P6	10.56	3.02	7.54
P7	12.10	5.08	7.02
P8	8.810	2.41	6.4
P9	10.11	2.03	8.08
P10	12.35	3.05	9.3
RMS = √405.97 = 20.14 cm			

4.9 ***I have measured the mean velocities of ground-surface deformation during the study period between 16 October 2018 and 21 March 2019 using PSI technique based on Sentinel-1 data for northwest Syria.*** 23,528 persistent scatterers were generated showing mean velocities of ground-surface deformations ranged from -47.70 mm per year to 101.64 mm per year in the satellite LOS direction during the study period (Figure 9) (Hammad et al., 2020).

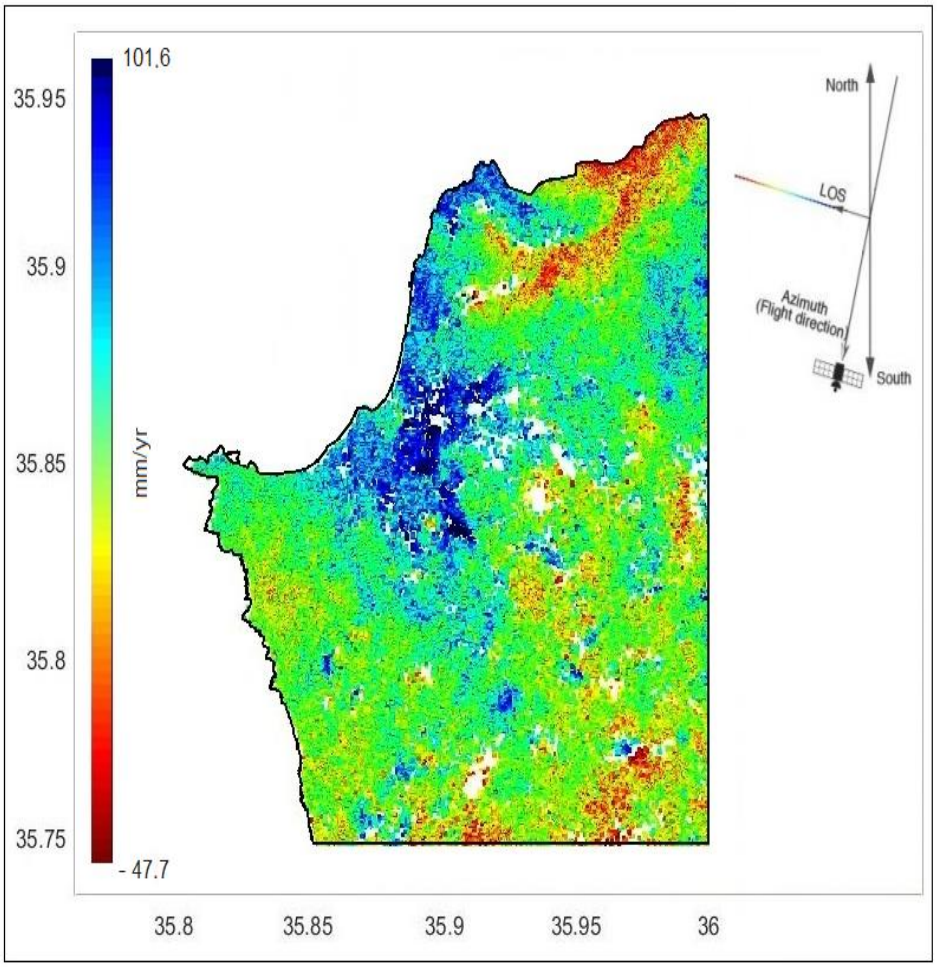

Figure 9: The persistent scatterer distribution map with mean velocities of ground-surface deformations in the LOS direction.

4.10 ***I have integrated the landslide susceptibility results of the ANN statistical analysis and the mean velocity results of the PSI technique using the landslide hazard matrix with the help of the GIS, which has proven to be a promising method of assessing landslide hazards using free SAR data and provides important results along the road network (Figure 5) (Hammad et al., 2020).*** The landslide susceptibility results and the mean velocities of ground-surface deformations resulting from the PSI technique have been classified into low-medium-high zones in order to be used in the landslide hazard matrix to assess the landslide hazard. As a result, the first landslide hazard map for northwest Syria was created as well as the spatial distribution of the three landslide hazard zones along the road network there (Figure 10). Moreover, two sites with a high hazard for landslides have been identified along the highway in the study area at Al-Qara'niya and Qastal Maaf (Figure 11). The results of the landslide hazard assessment need to be regularly updated to identify possible future landslide sites where the necessary precautions need to be taken to avoid losses and minimize the risk at these sites.

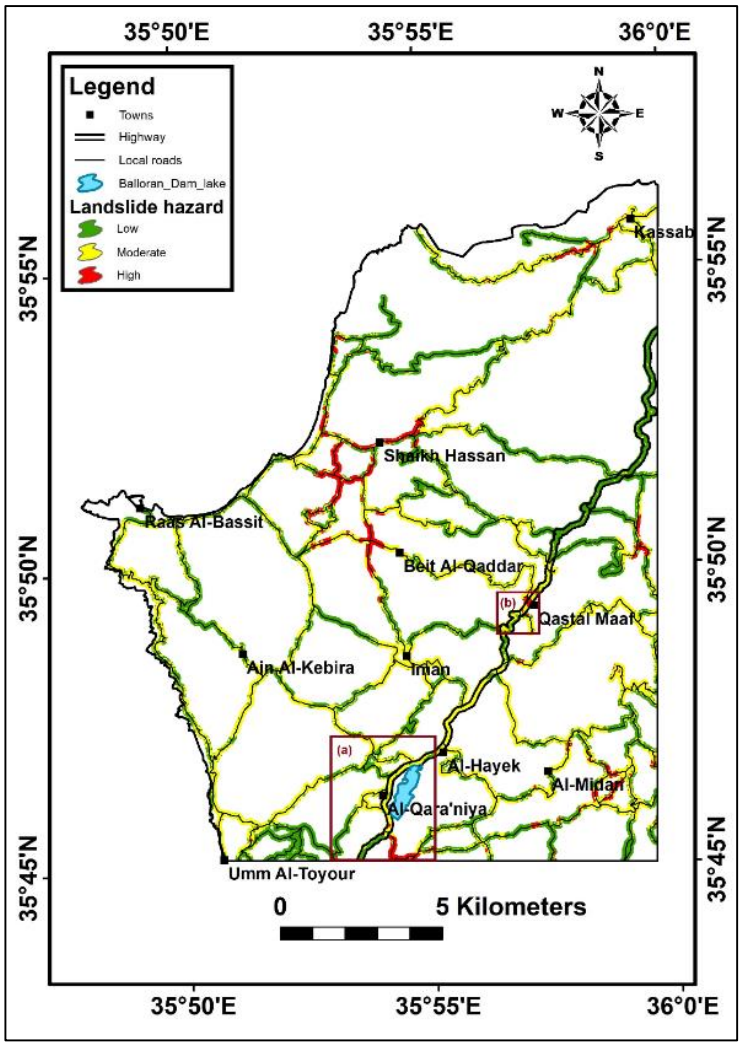

Figure 10: The spatial distribution of the three landslide hazard zones along the road network and the location of the two high hazard sites for landslides along the highway during the main 2018/2019 rainfall season.

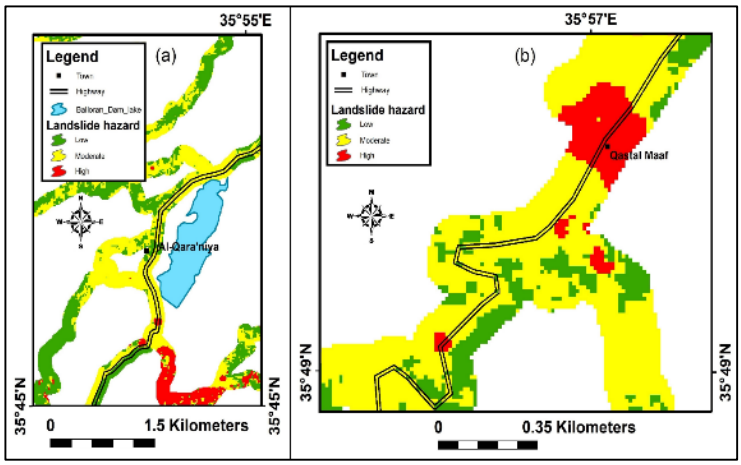

Figure 11: The two sites with a high hazard for landslides along the highway during the main rainfall season of 2018/2019.
a- The Al-Qara'niya site. b- The Qastal Maaf site.

Publications in relation to the dissertation

Hammad, M., Van Leeuwen, B. and Mucsi, L. (2017). Generation of DEMs of the Syrian coastal mountains from Sentinel-1 data. In: Balázs, B. (ed.), The 8th conference of theory meets practice in GIS. Debrecen, Hungary, 133-137.

Hammad, M., Van Leeuwen, B. and Mucsi, L. (2018a). Land Cover Change Investigation in the Southern Syrian Coastal Basins During the Past 30-Years Using Landsat Remote Sensing Data. Journal of environmental geography, 11(1), 45-51.

Hammad, M., Van Leeuwen, B. and Mucsi, L. (2018b). Ground- surface deformation investigation in Paks NPP area in Hungary using D-InSAR and PSI techniques. In: Molnár, V. (ed.), The 9th conference of theory meets practice in GIS. Debrecen, Hungary, 129-136.

Hammad, M., Mucsi, L. and Van Leeuwen, B. (2019). Landslide investigation using differential synthetic aperture radar interferometry: A case study of Balloran dam area in Syria. International Archives of the Photogrammetry, Remote Sensing and Spatial Information Sciences - ISPRS Archives, 42(3/W8), 133-138.

Hammad, M., Van Leeuwen, B., and Mucsi, L. (2020). Integration of GIS and advanced remote sensing techniques for landslide hazard assessment: a case study of northwest Syria. ISPRS Annals of the Photogrammetry, Remote Sensing and Spatial Information Sciences, 6(3/W1-2020), 27-34.